CHAPTER 4

APPLICATION OF "BALANCED ARCH" TECHNIQUE TO MGS ACCELEROMETER DATA

4.1 Introduction

I have used this technique to derive wind speeds from most of the MGS aerobraking profiles. Profiles with periapses poleward of 60° latitude or equatorward of 30° latitude were not used, as discussed in Section 3.3. As discussed by Tolson et al. (1999), there are some orbits in the ACC dataset that show unusual behaviour such as apparently constant density over significant changes in altitude. Strange phenomena of this nature may mean that the density data in this spot are bogus. If they are not bogus, then some of the assumptions that went into developing this technique are probably be invalid for that orbit, which makes the derived zonal wind speed very unrepresentative of the actual wind speeds in the atmosphere. These profiles have not been studied in great detail by anyone yet, so they probably contain lots of interesting behaviour that should cause individual orbits to be rejected. I discuss results from groups of orbits, averaging them together, so I hope that individual strange orbits do not bias the averaged results. Much work remains to be done to catalogue and understand all the small-scale phenomena in the ACC dataset.

The MGS ACC dataset is not published in the spherical polar coordinate system that I am working in. The MGS ACC PDS dataset uses altitude above a reference surface, aerocentric latitude, and aerocentric longitude as its three spatial coordinates (Keating et al., 2001a). The altds.cat file states that the "altitude is

above the IAU reference ellipsoid, with a=3393.4 km and f=0.0052083 and including corrections for (4,4) gravitational potential" (Keating et al., 2001a). This means that the reference surface is not actually an IAU reference ellipsoid. It is instead a fourth degree and order equipotential surface. Unfortunately, the archive does not state the coefficients that define the equipotential surface.

Such an equipotential surface is defined by a reference radius, a rotation rate, and many coefficients. Here I outline how a published set of coefficients can be related to the formula defining the surface. The total potential is the sum of gravitational and rotational potentials.

$$U = \frac{GM}{r}\left(1 + \sum_{l=2}^{l=\infty}\sum_{m=0}^{m=l}\left(\frac{r_{ref}}{r}\right)^{l}\bar{P}_{lm}\left(\cos\theta\right)\left(\bar{C}_{lm}\cos m\phi + \bar{S}_{lm}\sin m\phi\right) + \frac{r^3\Omega^2\sin^2\theta}{2GM}\right) \tag{4.1}$$

Where $\bar{P}_{lm}$ is the normalized associated Legendre polynomial of lth degree and mth order, $\bar{C}_{lm}$ is the normalized tesseral harmonic coefficient of lth degree and mth order, and $\bar{S}_{lm}$ is the normalized sectorial harmonic coefficient of lth degree and mth order. The equipotential surface $r_{ep}\left(\theta,\phi\right)$ has $U = U_{ep}$. For this equipotential surface I chose $U_{ep} = GM/r_{ref}$ and use $r_{ep} = r_{ref} + \delta r$:

$$\frac{GM}{r_{ref}} = \frac{GM}{r_{ref}+\delta r}\left(1 + \sum_{l=2}^{l=\infty}\sum_{m=0}^{m=l}\left(\frac{r_{ref}}{r_{ep}}\right)^{l}\bar{P}_{lm}\left(\cos\theta\right)\left(\bar{C}_{lm}\cos m\phi + \bar{S}_{lm}\sin m\phi\right) + \frac{r_{ep}^3\Omega^2\sin^2\theta}{2GM}\right) \tag{4.2}$$

Since $\delta r \ll r_{ref}$:

$$\frac{\delta r}{r_{ref}} = \sum_{l=2}^{l=\infty} \sum_{m=0}^{m=l} \bar{P}_{lm}(\cos\theta)\left(\bar{C}_{lm}\cos m\phi + \bar{S}_{lm}\sin m\phi\right) + \frac{r_{ref}^3 \Omega^2 \sin^2\theta}{2GM} \tag{4.3}$$

The normalization convention is important.

$$\bar{P}_{lm}(x) = N_{lm} P_{lm}(x) \tag{4.4}$$

Where N_{lm} is given by:

$$N_{lm} = \left((2-\delta_{lm})(2l+1)\frac{(l-m)!}{(l+m)!}\right)^{1/2} \tag{4.5}$$

And $P_{lm}(x)$ is given by:

$$P_{lm}(x) = \left(1-x^2\right)^{m/2} \frac{d^m}{dx^m} P_l(x) \tag{4.6}$$

Where $P_l(x)$ is the Legendre polynomial of lth degree and is given by:

$$P_l(x) = \frac{1}{2^l l!}\frac{d^l}{dx^l}\left(x^2-1\right)^l \tag{4.7}$$

This definition of $P_l(x)$ has the property that $P_l(1) = 1$. This normalization of the associated Legendre ploynomials is consistent with that of Kaula (1966) and many subsequent publications. The harmonic coefficients used in the MGS ACC PDS dataset were provided to me by Bob Tolson (personal communication, 2002). The reference radius in this case was 3382.4 km. These harmonic coefficients are consistent with those in Lemoine et al. (2001) which used a reference radius of 3397 km.

To transform PDS altitudes, z, into radial distances, r, I used $r = r_{ep}(\theta, \phi) + z$. Aerocentric latitudes, l_c, were transformed into aerographic latitudes, l_g, as follows:

$$\tan(l_c) = (1 - f)^2 \tan(l_g) \tag{4.8}$$

Colatitudes, θ, are simply $90° - l_c$. Aerocentric longitudes and aerographic longitudes, ϕ are identical.

The break between inbound and outbound legs where the pressure profiles are required to match is somewhat arbitrary. In deriving zonal wind speeds, I set this break at the minimum radial distance along the profile. This is not necessarily the same as the minimum altitude above the spatially varying equipotential surface nor as the minimum value of either of the two altitude scales in the PDS archive. The PDS archive has different altitude scales for 7s and 40s density averages.

In the discussions that follow, periapsis altitudes quoted for individual aerobraking passes are those taken from the PDS constant altitude dataset (Keating et al., 2001b). Where I have used periapsis altitude to select subsets of data, I also used this source for the periapsis altitude. I tend to group data by periapsis altitude, not by radial distance, because atmospheric conditions at the same altitude above the equipotential surface should be more similar than those at the same radial distance. This is because changes in gravitational potential have a greater effect on a parcel of atmosphere than mere changes in radial distance.

Formal uncertainties in zonal wind speed, as discussed in Section 3.7, are about 6 m s^{-1} for a typical aerobraking pass. These uncertainties are significantly smaller than the range in any subset of the derived zonal wind speeds from orbits which might be expected (similar latitude, longitude, altitude, *etc.*) to have the same winds. This range represents the effects of weather and the neglected terms. Accordingly, I treat the mean of a subset of derived zonal wind speeds as the

background zonal wind speed. Since the range in the data subset is much greater than any formal uncertainty on an individual zonal wind speed from one aerobraking pass, I use the unweighted mean:

$$< v >= \frac{1}{N} \sum_{i=1}^{i=N} v_i \tag{4.9}$$

The standard deviation of the distribution of zonal wind speeds is:

$$\sqrt{\frac{1}{N-1} \sum_{i=1}^{i=N} (v_i - < v >)^2} \tag{4.10}$$

The standard deviation of the mean of the zonal wind speeds is (Bevington, 1969):

$$\frac{1}{\sqrt{N}} \sqrt{\frac{1}{N-1} \sum_{i=1}^{i=N} (v_i - < v >)^2} \tag{4.11}$$

I use the standard deviation of the mean to test whether two subsets of data are different. If the mean plus its standard deviation in one data subset overlaps with the mean minus its standard deviation in another data subset, then I consider the two data subsets to be indistinguishable. If they do not overlap, then I consider them to be different.

4.2 Hemispheric Averages

Due to the complicated changes in MGS's orbit, data from Phase 2 of aerobraking and dayside LSTs are best for grouping aerobraking passes with similar parameters and the chance of building up reasonable statistics on the background zonal wind

speed. I first split the derived wind speeds into the two hemispheres, northern (NH) and southern (SH).

The NH orbits have L_s of 30° to 50°, periapsis latitudes of 60° to 30°N, and LSTs of 16.7 to 15.6 hrs. Most periapsis altitudes are between 111 and 118 km, with nine higher periapses at the start of this phase of aerobraking. Longitudinal coverage is good. With 149 orbits, the mean zonal wind speed is -74 m s^{-1} with an uncertainty of 5 m s^{-1}. Note that negative wind speeds are westward, or easterly, and blow from east to west.

The SH orbits have L_s of 75° to 85°, periapsis latitudes of 30° to 60°S, and LSTs of 14.7 to 14.8 hrs. All periapsis altitudes are between 104 and 114 km, and longitudinal coverage is good. With 100 orbits, the mean zonal wind speed is 34 m s^{-1} with an uncertainty of 7 m s^{-1}. Positive wind speeds are eastward, or westerly, and blow from west to east.

The derived zonal wind speeds in the NH are almost all negative and the standard deviation of their distribution is 62 m s^{-1}. The derived zonal wind speeds in the SH are mostly positive, but there are numerous negative results, and the standard deviation of their distribution is 71 m s^{-1}.

To learn how these derived zonal wind speeds vary with latitude, altitude, and longitude in each hemisphere, I examined subsets of the data where two of those parameters could be restricted and the other allowed to vary in a controlled way. Since the ACC data collection was motivated by the desire for the spacecraft to reach its mapping orbit, and not by any desire to maximize the scientific return of this engineering instrument, I was not always able to study these trends well.

4.3 Northern Hemisphere

4.3.1 NH — Effects of Longitude

I only consider orbits from the dayside of Phase 2 aerobraking with periapsis latitudes between 30° and 45°N and periapsis altitudes between 113 and 114 km. I shall show later in Section 4.3.2 that there is no significant variation in derived zonal wind speed with latitude in this range.

Results are shown in Table 4.1. With 60° wide longitude bins, only the 60–120°E (-145 m s^{-1}) and 180–240°E (-75 m s^{-1}) results can be statistically distinguished from each other, and not by very much. This is not strong evidence for variations with longitude, especially in comparison to the later latitude and altitude results for the NH (Sections 4.3.2 and 4.3.3). If I expand the longitude bins to 90° wide, then there are six or more measurements in each bin and all the results are statistically indistinguishable from each other. I conclude that there is no evidence for longitudinal variation in zonal wind speed in the NH.

4.3.2 NH — Effect of Latitude

I only consider orbits from the dayside of Phase 2 aerobraking with periapsis altitudes between 113 and 114 km. As Section 4.3.1 has shown that there is no significant effect of periapsis longitude on derived zonal wind speed in the dayside Phase 2 data, I do not impose any constraints on periapsis longitude. Results are shown in Table 4.2. Using 5° wide latitude bins, I see that the derived zonal wind speed becomes less negative (slower but still westward) as periapsis latitude increases to the north. This can be seen more clearly if the data are split into just two latitude bins with the boundary at 43°N.

Lon. Range (°E)	Mean v_ϕ (m s^{-1})	σ of Dist. (m s^{-1})	σ of Mean (m s^{-1})	N
0–60	-74	86	43	4
60–120	-145	76	44	3
120–180	-87	39	15	7
180–240	-75	41	18	5
240–300	-67	65	46	2
300–360	-90	93	31	9
0–90	-84	71	29	6
90–180	-104	61	22	8
180–270	-72	43	16	7
270–360	-90	93	31	9

Table 4.1: NH — Effects of Longitude

Lat. Range (°N)	Mean v_ϕ (m s^{-1})	σ of Dist. (m s^{-1})	σ of Mean (m s^{-1})	N
30–35	-78	66	20	11
35–40	-106	69	23	9
40–45	-85	75	24	10
45–50	-43	45	18	6
30–43	-95	70	14	26
43–50	-43	39	12	10

Table 4.2: NH — Effects of Latitude

4.3.3 NH — Effect of Altitude

I only consider orbits from the dayside of Phase 2 aerobraking with periapsis latitudes between 30° and 50°N. As Section 4.3.1 has shown that there is no significant effect of periapsis longitude on derived zonal wind speed in the dayside Phase 2 data, I do not impose any constraints on periapsis longitude. Results are shown in Table 4.3. Zonal wind speed becomes more negative (the winds are faster and more westward) as altitude increases. This can be seen more clearly if the middle altitude sections are combined. The surprisingly large change in derived zonal wind speed over 5 km is discussed in Section 4.5.

4.3.4 NH — Summary

The mean zonal wind speed from the dayside of Phase 2 aerobraking is -74 m s^{-1} with an uncertainty of 5 m s^{-1}. No variation in zonal wind speed with longitude was observed, zonal wind speed became more negative as altitude increased, and zonal wind speed became less negative as latitude increased northward.

4.4 Southern Hemisphere

4.4.1 SH — Effect of Longitude

The significant change in periapsis altitude with change in periapsis latitude during this part of aerobraking prevents me from repeating the approach of Section 4.3.1 here. Instead, I study a smaller subset of data which is more suited to studying the effects of longitude, but which does not have as many orbits per longitude bin as Section 4.3.1. The orbital period of MGS decreased on each orbit due to the effects of atmospheric drag. At the start of aerobraking it was over 30 hours long, at the end of aerobraking it was less than two hours long. Whenever the orbital period was a submultiple of Mars's 24.6 hour rotational period, periapsis longitude was repeated

Alt. Range (km)	Mean v_ϕ (m s^{-1})	σ of Dist. (m s^{-1})	σ of Mean (m s^{-1})	N
111–112	-40	52	14	13
112–113	-73	62	13	24
113–114	-81	67	11	36
114–115	-72	68	16	18
115–116	-96	56	17	11
111–112	-40	52	14	13
112–115	-76	65	7	78
115–116	-96	56	17	11

Table 4.3: NH — Effects of Altitude

at intervals of one martian day. Changes in periapsis latitude and altitude were usually small over this interval, so orbits during this short-lived "resonance period" provide several derived zonal wind speeds at very restricted latitudes, altitudes, and longitudes.

The 8:1 resonance spans orbits 1030–1057 and periapsis latitudes of 41–49°S. Results are shown in Table 4.4. Longitude is correlated with periapsis altitude due to the orbital dynamics and shape of Mars, so there are two slightly different sets of data here — high and low. "High" orbits have periapsis altitudes of 109–110 km, and "low" orbits have periapsis altitudes of 108–109 km. The number of measurements in each longitude bin is equal to the number of periapsis altitudes in the last column of Table 4.4. I have discarded a few orbits from this resonance to make sure that each longitude bin has a range in periapsis altitude of no more than 1.2 km. Comparing derived zonal wind speeds from the 20°E and 335°E longitude bins or 245°E and 290°E longitude bins makes it clear that significant longitudinal variations exist in the SH zonal winds.

4.4.2 SH — Effect of Latitude

I only consider orbits from the dayside of Phase 2 aerobraking with periapsis latitudes between 30° and 50°S and periapsis altitudes between 108 and 110 km. If I do not impose any constraints on periapsis longitude, then there are no statistically significant changes in zonal wind speed with latitude. If I try to restrict periapsis longitude in some way and compare derived zonal wind speeds from one latitude/longitude/altitude bin to another with the same altitude and longitude, but different latitude, then it is difficult to find enough orbits to generate meaningful statistics. This is because periapsis altitude and periapsis latitude change together during this part of aerobraking. As periapsis latitude precessed towards the south pole and the atmosphere became colder and less dense, periapsis altitude was decreased by the mission operations team to maintain the same periapsis

Lon. (°E)	Mean v_ϕ (m s^{-1})	σ of Dist. (m s^{-1})	σ of Mean (m s^{-1})	Peri. Alts. (km)
20	-55	63	36	110.0, 109.5, 108.8 (high)
65	18	72	42	108.8, 108.3, 107.6 (low)
110	62	50	29	109.2, 108.6, 108.2 (low)
155	86	37	21	110.0, 109.4, 108.8 (high)
200	-49	35	25	110.5, 109.4 (high)
245	70	41	24	109.0, 108.5, 107.9 (low)
290	7	36	21	108.8, 108.3, 108.0 (low)
335	122	38	22	110.2, 109.7, 109.2 (high)

Table 4.4: SH — Effects of Longitude

density.

Results are shown in Table 4.5. Extreme variations with longitude are seen at 30–35°S. Two longitude bins show derived zonal wind speeds becoming more positive, with statistical significance, as latitude moves southward, and one (0–120°E) shows more negative zonal wind speed as latitude moves southward, though without statistical significance. These data hint at generally more positive zonal wind speed as periapsis latitude moves southward, but it is not able to test this hypothesis well.

4.4.3 SH — Effects of Latitude and Altitude

I only consider orbits from the dayside of Phase 2 aerobraking with periapsis latitudes between 35° and 60°S. Periapsis altitude (which ranges between 104 and 114 km) is not used to discard any orbits. Periapsis latitudes between 30° and 35°S are not considered because they do not follow the trend of periapses moving poleward and downward simultaneously. I split the remaining data into two parts by either which side of 108 km or which side of 50°S it falls on. The two splitting techniques give exactly the same results. Four longitude bins, each 90° wide, are considered. Results are shown in Table 4.6.

I show in the table the mean derived zonal wind speed ± the standard deviation of the mean for the relevant subsets of data. Values are rounded to the nearest 10 m s^{-1} in this table only to highlight the major trends. On each side of the split, the four longitude bins have similar means and standard deviations for altitude and latitude. Longitudinal differences cannot be caused by differences in the latitudinal or vertical distribution that was sampled by each longitudinal bin. All the longitude bins contain more than 10 data points. Derived zonal wind speeds become more positive as periapsis altitude decreases/latitude moves southward for two of the four longitude bins, but in the remaining two it stays constant. There are longitudinal differences both in the value of the derived zonal wind speed at any

Lat. Range (°S)	Mean v_ϕ (m s^{-1})	σ of Dist. (m s^{-1})	σ of Mean (m s^{-1})	N
30–35 (0–360° E)	20	110	33	11
40–50 (0–360° E)	47	66	13	24
30–35 (0–120° E)	99	112	56	4
30–35 (120–240° E)	-68	115	67	3
30–35 (240–360° E)	7	51	26	4
40–50 (0–120° E)	25	72	23	10
40–50 (120–240° E)	63	56	25	5
40–50 (240–360° E)	62	64	21	9

Table 4.5: SH — Effects of Latitude

Lon. Range (°E)	High and North	Low and South
0–90	0 ± 20	0 ± 20
90–180	20 ± 20	40 ± 20
180–270	0 ± 20	60 ± 20
270–360	60 ± 20	60 ± 20

Table 4.6: SH — Effects of Latitude and Altitude

given latitude and in how this value changes with latitude/altitude. This reinforces the results of Section 4.4.1 that longitude is an important factor in the SH zonal wind speeds.

This result was unexpected. Why is there such longitudinal variability in the southern, but not the northern, hemisphere? Are the longitudinal variations in derived zonal wind speed related to longitudinal variations in density?

4.4.4 SH — Summary

The mean zonal wind speed is 34 m s^{-1} with an uncertainty of 7 m s^{-1}. Extensive variation in zonal wind speed with longitude was observed. Zonal wind speeds became more positive as altitude decreased/latitude moved southward for some longitude bins, but stayed constant in others. Altitude and latitude are coupled in the data, which makes it difficult to separate their effects.

4.5 Discussion of Results

It is unfortunate that I have not been able to validate this technique on an actual dataset. With one exception, all the zonal wind speeds that I have derived above seem physically plausible. The exception is in Section 4.3.3 where the zonal wind speed doubles over a change in altitude of 5 km, less than a scale height. If this is not an accurate representation of the atmosphere, what is it? Measurements made between 111 and 112 km in this Section have very different results than those in any other 1 km wide altitude range in Table 4.3. Measurements in this altitude range are predominantly collected towards the north of the 30 – 50°N latitude band. As was shown in Section 4.3.2, the northern third of this latitude band has quite different derived zonal wind speeds from the southern two-thirds. Section 4.3.3 may have misattributed changes due to latitude to altitude. While I have tried to mitigate that problem by careful selection of subsets of data, it is not possible to eliminate it.

Two subsets of data never have exactly the same population of latitude, longitude, and time (meaning date/time of measurement, which might be important if the weather is windy for a few days and then quiet for the next few days) to permit study of the effects of altitude without any interference from other effects.

I believe that the hemispherically averaged wind speeds are robust. They include over 100 data points in each hemisphere, which should be sufficient to smooth out variations due to longitude and altitude. Sections 4.4.1 and 4.4.3 have used two different approaches to discover that longitudinal variations are important in the southern hemisphere. My work on variations in zonal wind speed with latitude within a hemisphere, with altitude over a range less than a scale height, and with longitude in the northern hemisphere has not convinced me that any of these suggested trends are free from all interference.

4.6 Comparison to Simulations

No observations exist that can be compared to my results for the zonal wind speed in the martian upper atmosphere. Instead, I compare my results to simulations from a General Circulation Model (MTGCM) (Bougher et al., 1999).

Results from MTGCM simulations relevant for the northern hemisphere work are shown in Figure 4.1 and for the southern hemisphere work in Figure 4.2. My derived zonal wind speed of -74 m s^{-1} for the northern hemisphere between 30 and 60°N and 111 to 118 km is very different from the MTGCM value of 20 – 40 m s^{-1}. My derived zonal wind speed of 34 m s^{-1} for the southern hemisphere between 30 and 60°S and 104 to 114 km is also somewhat different from the MTGCM value of 60 – 100 m s^{-1}, but the discrepancy is less.

In both Section 4.3.2 and Figure 4.1 the zonal wind speed becomes more positive as latitude increases northward. The simulated zonal wind speed in Figure 4.1 barely changes with altitude at all. This is not consistent with the 111 – 112

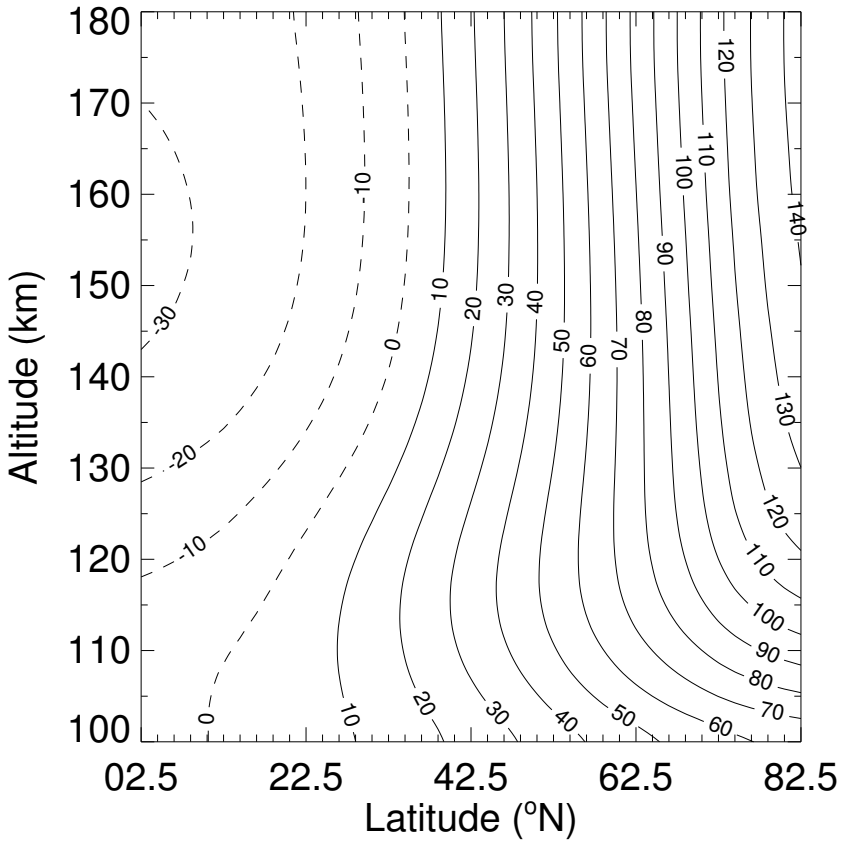

Figure 4.1: Zonal wind speed (m s^{-1}) from an MTGCM simulation relevant for $L_s = 30°$, LST = 16 hrs. Solid contours are positive (eastward) zonal winds, dashed contours are negative (westward).

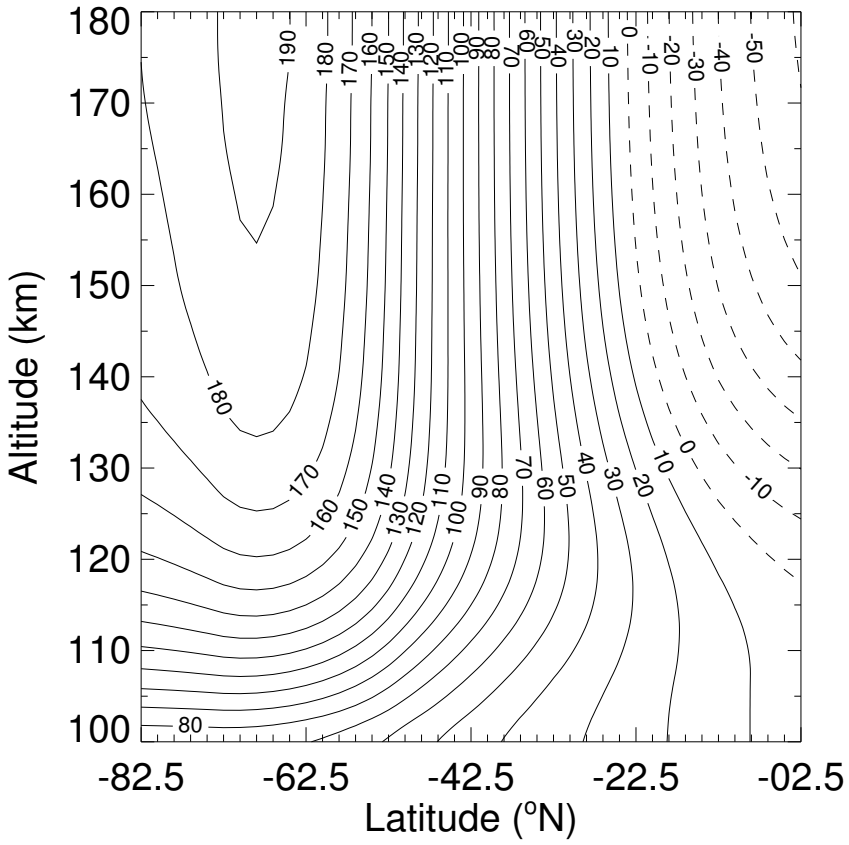

Figure 4.2: Zonal wind speed (m s^{-1}) from an MTGCM simulation relevant for $L_s = 90°$, LST = 15 hrs. Solid contours are positive (eastward) zonal winds, dashed contours are negative (westward).

km data discussed in Section 4.3.3, but is consistent with the other altitude bins. As discussed in Section 4.5 the 111 – 112 km data may not be representative of the effects of altitude after all.

In Section 4.4.2 the data hint at the zonal wind speed becoming more positive as latitude trends southward. This is consistent with Figure 4.2. Averaged over all longitudes, Section 4.4.3 does not show any great difference between winds speeds above 108 km and north of 50°S and wind speeds below 108 km and south of 50°S. This is consistent with Figure 4.2 in which the wind speed contours slope in the correct direction to give no great change in wind speed between these two conditions.

The MTGCM simulations shown here are not capable of studying the effects of longitude since they are zonally averaged. Of the three results that I am most comfortable with from this work, one (SH longitude) cannot be compared to the MTGCM simulations, one (NH average) differs from the simulations by 100 m s^{-1}, and the other (SH average) differs from the simulations by 30 m s^{-1}. Since the wind speeds predicted in the simulations have never been compared to direct observations, it is difficult to know which is most likely to be correct. MTGCM simulations with detailed coupling to a lower atmosphere model are in progress and preliminary results show that winds are significantly affected by zonal averaging and that results are very sensitive to the atmospheric dust distribution.

4.7 Future Work

The "Balanced Arch" technique originated in my desire to derive pressure and temperature profiles from the MGS ACC data using the same techniques that have been applied to density profiles from landers and entry probes. I have shown that winds complicate this significantly. There are many assumptions that have been made to derive this technique, more than I would like. This technique needs to be applied to GCM simulations to see how robust it is. I would also like to apply it

to some real data, which include weather and other transient phenomena which are not present in the GCM. A suitable dataset from Mars is not likely to arrive in the near future. Maybe terrestrial measurements at low geomagnetic activity levels are suitable for this testing.

However, since there are so few measurements of winds in atmospheres other than Earth, uncertain results are still scientifically useful. Even something as simple as knowing which way the wind blows in the martian upper atmosphere would be valuable. I have not presented any pressure or temperature profiles here. It may be that this technique does a reasonable job of obtaining the averaged pressure profile, but erases all small-scale structure. Or the opposite might be true. Either would be useful. There is much to study in derived pressure and temperature profiles, whatever technique is used to acquire them.

The Pathfinder entry profile is closer to vertical than an MGS aerobraking pass, but it still covers 1000 km of horizontal distance during a 200 km vertical descent. It would be interesting to use the results of this work to see how much uncertainty winds introduce into these, and the Viking, results. The Galileo entry profile may also be affected by this, but its measurements of winds with the Doppler Wind Experiment might provide a way to correct any errors.

If, after further study, I find that the "Balanced Arch" technique does work well in obtaining zonal wind speeds and pressure and temperature profiles, it will be easy to extend it to derive a vertical profile of zonal wind speed between the two legs of a single aerobraking pass. In this work I have concentrated on demonstrating the simplest possible implementation of my ideas as I think it is better to validate the concept before pushing it to its formal limits.